How Long should the MISR Record Be when Evaluating Aerosol Optical Depth Climatology in Climate Models?

Huikyo Lee [1,*,†] (ID), **Michael J. Garay** [1,†] (ID), **Olga V. Kalashnikova** [1] (ID), **Yan Yu** [2] (ID) **and Peter B. Gibson** [1] (ID)

1 Jet Propulsion Laboratory, California Institute of Technology, Pasadena, CA 91109, USA; michael.j.garay@jpl.nasa.gov (M.J.G.); olga.kalashnikova@jpl.nasa.gov (O.V.K.); peter.gibson@jpl.nasa.gov (P.B.G.)
2 Department of Geography, University of California, Los Angeles, CA 90095, USA; yuyan06@gmail.com
* Correspondence: huikyo.lee@jpl.nasa.gov; Tel.: +1-818-354-7411
† These authors contributed significantly to this work.

Abstract: This study used the nearly continuous 17-year observation record from the Multi-angle Imaging SpectroRadiometer (MISR) instrument on the National Aeronautics and Space Administration (NASA) Terra Earth Observing System satellite to determine which temporal subsets are long enough to define statistically stable speciated aerosol optical depth (AOD) climatologies (i.e., AOD by particle types) for purposes of climate model evaluation. A random subsampling of seasonally averaged total and speciated AOD retrievals was performed to quantitatively assess the statistical stability in the climatology, represented by the minimum record length required for the standard deviation of the subsampled mean AODs to be less than a certain threshold. Our results indicate that the multi-year mean speciated AOD from MISR is stable on a global scale; however, there is substantial regional variability in the assessed stability. This implies that in some regions, even 17 years may not provide a long enough sample to define regional mean total and speciated AOD climatologies. We further investigated the agreement between the statistical stability of total AOD retrievals from MISR and the Moderate Resolution Imaging Spectroradiometer (MODIS), also on the NASA Terra satellite. The difference in the minimum record lengths between MISR and MODIS climatologies of total AOD is less than three years for most of the globe, with the exception of certain regions. Finally, we compared the seasonal cycles in the MISR total and speciated AODs with those simulated by three global chemistry transport models in the regions of climatologically stable speciated AODs. We found that only one model reproduced the observed seasonal cycles of the total and non-absorbing AODs over East China, but the seasonal cycles in total and dust AODs in all models are similar to those from MISR in Western Africa. This work provides a new method for considering the statistical stability of satellite-derived climatologies and illustrates the value of MISR's speciated AOD data record for evaluating aerosols in global models.

Keywords: MISR; speciated AODs; speciated AOD climatologies; statistical stability of total and speciated AOD climatologies

1. Introduction

Aerosols exert considerable impacts on air quality and the Earth's radiation budget, yet neither their mean state in the current climate nor their response to a changing climate are well represented in global climate models [1]. In recent years, there have been many studies evaluating the aerosol optical depth (AOD) simulated by climate models using satellite observations. Assessing the mean

AOD in models may be the most fundamental task for evaluating the direct and indirect radiative effects of aerosols in the models (e.g., Shindell et al. [2], Park et al. [3], Pan et al. [4], Zhu et al. [5]). Most of these studies considered the multi-year mean AODs derived from satellite observations as their reference datasets. In spite of the fact that satellite-derived AODs have been widely used as a proxy for climatological AOD, it is currently unknown how many years of an AOD dataset are required to generate a statistically stable mean AOD "climatology". Indeed, the use of satellite-derived AOD climatologies for benchmarking climate models has been performed based more on the availability of datasets and temporal overlap with available model runs, rather than any objective standards.

The World Meteorological Organization (WMO) defines "climate" as the system's state averaged over 30 years. Loew [6] demonstrated that the length of precipitation and vegetation data record from satellite observations strongly affects the calculation of temporal trends and the correlation between the variables. Long data records are also important due to the existence of observed decadal-scale modes in the climate system, such as the Pacific Decadal Oscillation [7]. However, reliable AOD datasets over both land and ocean from instruments on the National Aeronautics and Space Administration's (NASA's) Earth Observing System (EOS) satellites became available only in early 2000. Currently, the longest record of AOD from EOS observations spans just over 18 years.

As more AOD data from satellites become available, different studies use different averaging periods to define what they consider to be an appropriate AOD climatology. For example, AODs averaged for five and nine years were defined as the aerosol climatology in Remer et al. [8] and Sreekanth [9] respectively. Pan et al. [4] used satellite-derived AOD averaged for the eight years between 2000 and 2007. The six-year mean AOD between 2000 and 2005 was compared with model simulations in Misra et al. [10]. More recent studies define AOD climatologies as the mean of AOD over a longer period of time than 10 years. In Aklesso et al. [11], the AOD climatology is an averaged AOD between 2005 and 2015. Kumar et al. [12] investigated the mean and variability of AOD over Kazakhstan between 2003 and 2015. In Boiyo et al. [13], Hu et al. [14], AOD climatologies represent temporally averaged AOD for the 14 years between 2002 and 2016. Even so, these inconsistent uses of the concept of an AOD "climatology" based on satellite observations along with the significant interannual variability in AOD reported in many studies (e.g., Lee et al. [15]) identify a clear and urgent need to objectively quantify the sensitivity of multi-year mean satellite-derived AOD "climatology" to the length of the observation periods.

Recent studies have also shown that biases and uncertainties in model-simulated aerosol fields are still considerable, and there is little agreement in terms of aerosol composition among models. For example, the global mean AOD agreed to within about 20% when satellite observations were compared with ten climate chemistry models by Shindell et al. [2]. However, the models showed a much larger spread in AOD when stratified by different types of aerosols in the same study. Tsigaridis et al. [16] also showed that the amount and properties of organic aerosols can vary substantially among climate models. Because of the large variability in speciated AODs (i.e., AOD separated by particle types) in the climate models that contribute to international projects like the Aerosol Comparisons between Observations and Models (AEROCOM, Myhre et al. [17]), the upcoming Coupled Model Intercomparison Project Phase 6 (CMIP6, Eyring et al. [18]) and its endorsed sub-projects such as the Aerosols and Chemistry Model Intercomparison Project (AerChemMIP), it is a high priority to systematically evaluate simulated AODs for different types of aerosols against observational data. This further helps us assess the aerosol type information that is determined by the characteristics of different emission sources (e.g., anthropogenic emissions, wildfires, volcanoes, dust storms, etc.), and the resulting radiative forcing from individual aerosol types.

The main objectives of the present study are to provide guidance to the aerosol modeling and remote sensing communities on constructing and using so-called "climatological" AOD based on satellite observations averaged over multiple years, and to further examine the uncertainties in these multi-year mean AODs for different particle types. In this work, we considered the AOD and aerosol type information from the Multi-angle Imaging SpectroRadiometer (MISR, Diner et al. [19],

Diner et al. [20]) instrument, which has been operational on the NASA Terra EOS satellite since early 2000. We quantified the uncertainty in total and speciated AOD climatologies by calculating the standard deviation resulting from a random subsampling of 17 annual mean and seasonally averaged AODs. Because the statistical uncertainties increase as the sample sizes decrease, we examined variability of the uncertainty as a function of sampling lengths and determined minimum record lengths required for the observed total and speciated AODs from MISR to meet certain uncertainty levels. We performed the same analysis of the Moderate Resolution Imaging Spectroradiometer (MODIS) data for total AOD from the Terra satellite, which provides a similar basis for comparison. Of course, the approach can be extended to other satellite aerosol and non-aerosol datasets. Finally, in the current study, we also compared the MISR total and speciated AODs with the optical depths for total, sulfate, and dust aerosols in the three Global Aerosol Climatology Project (AEROCOM) Phase II hindcast simulations from the GOCART [21], HadGEM2 [22], and SPRINTARS [23] models.

2. Materials and Methods

MISR's nine cameras observe the Earth in four visible and near infrared (NIR) wavelengths (446.4 nm-blue, 557.5 nm-green, 671.7 nm-red, 866.4 nm-NIR) with a swath of approximately 400 km. The multi-angle viewing approach enables MISR to distinguish mixtures of different particle types over both land and ocean. MISR retrievals of total AOD and AOD for eight different particle types are available beginning in March 2000 [24,25]. Kahn et al. [24], Garay et al. [26] compared the total MISR AOD with the ground-based Aerosol Robotic Network (AERONET, Holben et al. [27]) observations and found that overall about 70–75% of the MISR AOD fall within the greater of 0.05 or 20% of the AERONET AOD. Especially over land and bright surfaces, MISR's AOD retrievals tend to show better performance compared with retrievals from other satellite instruments, so MISR AOD retrievals over land are currently used in the AEROCOM project [28] and Observations for Model Intercomparisons Project (Obs4MIPs) [29,30]. The eight particle types in the MISR algorithm climatology include four non-absorbing spherical particle optical analogs, two spherical absorbing particle analogs, and two non-spherical-particle size distributions corresponding to fine and coarse mode dust. Over the regions whose total AOD exceeds about 0.15, uncertainties in the MISR AODs by particle types are relatively small [24], so it is typically desirable to use the AODs by particle types from MISR near major sources of aerosol emissions [15,31].

To assemble our statistics, we utilized the seasonally and annually averaged AODs for all aerosols (hereafter referred to as total AOD), non-absorbing aerosols (non-absorbing AOD), absorbing aerosols (absorbing AOD), and non-spherical aerosols (non-spherical AOD) reported at a wavelength of 558 nm over the 17-year period from March 2000 through February 2017. The monthly mean AOD was calculated using the gridded Joint Aerosol Product Version F01_0001(JOINT_AS) [15]. The spatial resolution of the JOINT_AS product is 5° × 5°. There are other MISR aerosol products that provide total AOD and non-spherical AOD at a higher spatial resolution than JOINT_AS. However, JOINT_AS is the only MISR product that provides gridded AODs for the eight different particle types assumed in the retrieval algorithm. Figure 1 presents maps of the AODs for total, non-spherical, non-absorbing, and absorbing aerosols averaged over the entire time period. The major emission sources of the three particle types are well characterized. For example, the Sahara Desert is the largest source of non-spherical aerosols in the world (Figure 1b). Non-absorbing aerosols, such as sulfate and nitrate, are primarily emitted from anthropogenic sources in China and India (Figure 1c). Savanna grassland fires emit a large number of absorbing aerosols over Central Africa [32] and biomass burning sources in the Amazon and Indonesia are also apparent, along with anthropogenic sources of absorbing aerosols in China and India (Figure 1d). The non-spherical, non-absorbing, and absorbing AODs from JOINT_AS have been shown to be comparable to model-simulated AODs for sulfate aerosols, carbonaceous aerosols, and dust, respectively [15].
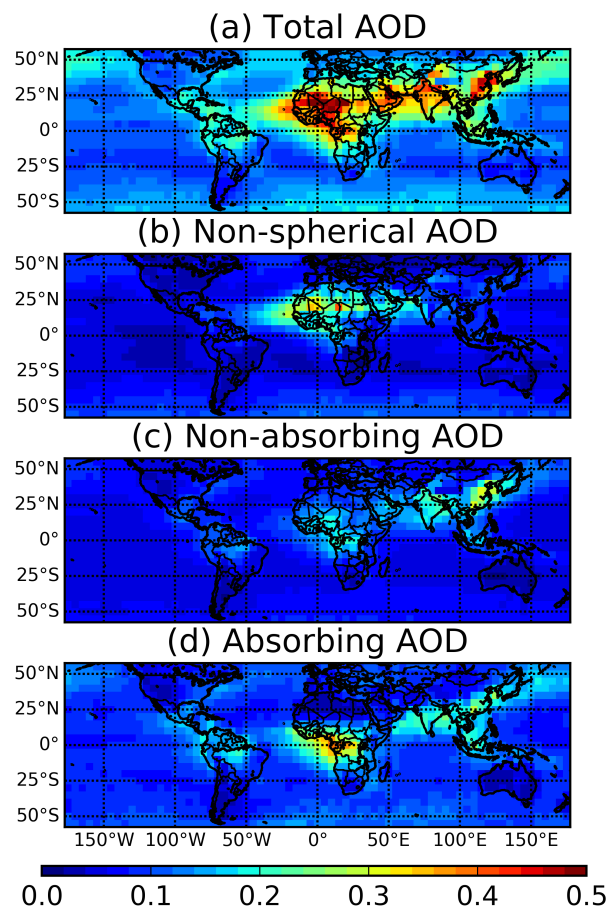
Figure 1. The 17-year mean optical depths of (**a**) total aerosols, (**b**) non-spherical aerosols, (**c**) non- absorbing aerosols, and (**d**) absorbing aerosols from the MISR JOINT_AS product.

Before moving to a quantitative analysis of climatological AODs, we assessed the representativeness of the seasonally and annually averaged AODs calculated in each year and identified patterns in 17-year time series. First, we found that the overall number of retrieved AODs used to calculate the monthly mean AOD does not exhibit a strong seasonal cycle when the globe is considered to be whole, but regional differences in sampling reflect seasonal changes in cloud cover (Figure A1). This indicates that the annual mean AOD, which is calculated using 12 monthly mean AODs, may represent each year's AOD and can, therefore, be used to examine the statistical stability of the climatological AOD. Next, we tested the statistical significance in the AOD trend (Figure A2) and the 1-year lag autocorrelation (Figure A3) in the time series of annual AOD at each $5° \times 5°$ grid point. Here, the trend corresponds to the slope of the least square line fitting the annual mean AOD time series. The test statistic to check statistical significance of the trend is a *t* statistic defined as the slope divided by its standard error. In this simple linear regression, we assumed that the degree of freedom is 15 ($n - 2$) at each grid point. (1-*p*-values) in % for the test statistic are displayed in Figure A2 as confidence levels for the trends. Statistically significant trends in the total and speciated AODs are found in some regions, including along the East Coast of the United States, over Europe, India, and the Arabian Sea. Significant trends in non-spherical AOD are seen over North Africa and over Japan, most likely due to transported dust. The confidence levels for 1-year lag autocorrelation, calculated using the Ljung-box test [33], also show some statistically significant locations over these same regions, but typically over much smaller areas. With the exception of the Arabian Sea, the 17-year mean AODs shown in Figure 1 tend to be relatively low in those regions with significant AOD trends. This implies

that most of the significant AOD trends are not associated with a large increase in atmospheric aerosol loading on a global scale.

To quantify the uncertainty in the multi-year mean AOD derived from MISR observations as a function of sampling period length, we randomly subsampled the seasonal or annual mean AOD for the 17 years without replacement. And a sample size varies between 1 and 16 years. For example, when the sample size equals 4, the randomly subsampled years can be the set 2000, 2001, 2005, and 2010, the set 2001, 2006, 2007, and 2016, or some other combination of years. For each sample size, the subsampling was repeated 1000 times. Sampling more than 1000 times had almost no influence on the results shown in the following sections. Then, using the 1000 subsampled datasets, we generated 1000 multi-year mean AODs and calculated their mean and standard deviation. A similar random sampling approach has been applied to evaluating hourly precipitation simulated by regional climate models using the observational datasets that do not have any temporal overlap with the simulations [34]. As an example, Figure 2 shows the mean and standard deviation of the total AOD climatology in boreal fall (September– November) across the 1000 samples for each sample size from 1 to 16 years. The AOD time series represents one grid point located in northeastern China (centered at 37.5° N, 117.5° E). In this case, the mean AOD based on 1000 subsamples does not exhibit large variability in the region if the sample size is greater than or equal to four years. In contrast, the standard deviations of subsampled mean AODs that quantify the uncertainty of climatological mean AOD are highly sensitive to the length of sample periods. For a sample size of one year, the standard deviation is 0.047, 12.9% of the 17-year mean AOD for the climatology (0.362). To obtain a multi-year AOD with a sample standard deviation less than 0.01, it is necessary to average at least 11 years of AODs at this grid point for the boreal fall season. The 0.01 AOD criterion is about 5% of the global mean AOD of 0.2, which is averaged with weighting by the cosine of latitude (to provide approximately equal area sampling) over land during the 17 years between March 2000 and February 2017. Please note that in this analysis, we treat the 17-year mean AOD as if it were the "true" climatology.
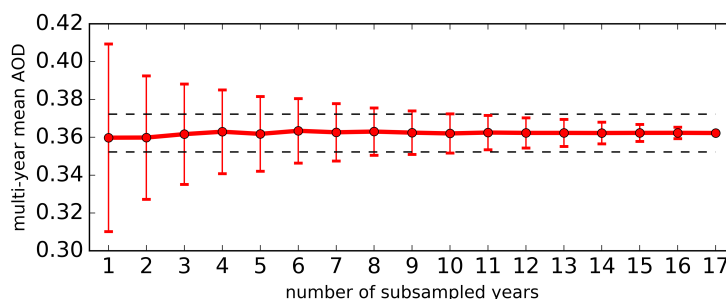

Figure 2. The red dots are averages of 1000 randomly subsampled multi-year mean AODs in northeastern China (37.5° N, 117.5° E) in boreal fall (from September through November) from random samples. The error bars represent uncertainties of multi-year seasonal mean AOD due to the temporal subsampling. The dotted lines present AOD values of 0.352 and 0.372 (±0.01 from the 17-year mean AOD of 0.362).

To test the validity of this approach, we also used the total AOD from MODIS for the same 17-year period. For this study, the MODIS Collection 6 Level 3 AOD over ocean and land at a horizontal resolution of 1° × 1° retrieved using the Dark Target [35] and Deep Blue [36] algorithms respectively, was used. The wider swath of MODIS, 2330 km compared to MISR's 400 km, assures better spatial coverage in the MODIS AOD product compared to that from MISR. To provide a more direct comparison, we further aggregated and averaged the higher resolution MODIS AOD dataset to the coarse 5° × 5° grids of the MISR JOINT_AS product. Note, however, that the MODIS AOD product does not contain the particle type information provided by the MISR aerosol retrieval.

3. Results

Figure 3a displays a map of the minimum MISR record lengths required for the sample standard deviation of the total AOD to be less than 0.01 for the annual mean climatology. Higher numbers indicate that a longer observation period is required to obtain a statistically stable AOD that agrees with the MISR-derived 17-year average. The minimum record length and the statistical stability of the subsampled multi-year mean AOD vary in opposite directions with longer record lengths corresponding to more highly variable annual mean AODs. Overall, the stability of multi-year mean total AOD shows substantial regional variability. Over the global ocean, the minimum required record length is about one year, but for certain locations over land, the minimum required record length can be up to 11 years. The Amazon, the central Congo, and Indonesia, well known major sources of biomass burning aerosols, are all locations that require long record lengths. The region around the Arabian Sea, frequently impacted by dust storms, and the industrial region of eastern China are also locations that require long record lengths to achieve statistical stability. Large interannual variability results in a large standard deviation for these areas, leading to a longer required record length. Because emissions from land account for most of atmospheric aerosols, the AOD climatology is more stable over ocean than over land with exception of ocean regions downwind of major dust sources, such as the eastern Atlantic Ocean between the equator and 30° N, the Indian Ocean off the Arabian Peninsula, and the downwind of East Asia.
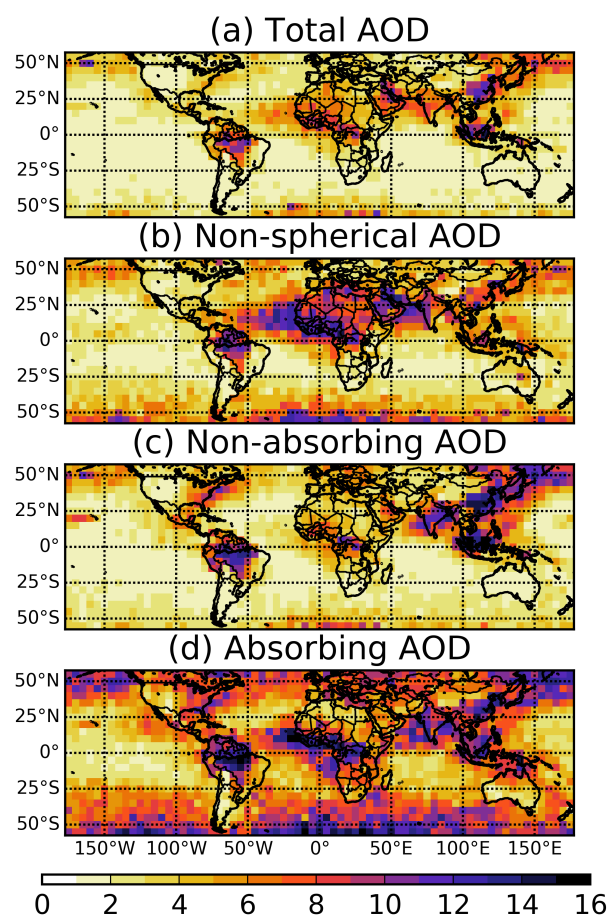

Figure 3. The minimum record lengths required to obtain stable annual mean climatology of (**a**) total, (**b**) non-spherical, (**c**) non-absorbing, and (**d**) absorbing aerosol optical depths within the predefined accuracy levels ±0.01 AOD for (**a**), ±0.004 for (**b**), and ±0.005 for (**c**) and (**d**).

The sensitivity of the AOD climatology to a sampling period becomes greater for the speciated AODs as shown in Figure 3. Please note that the mean and interannual variability of speciated AODs are also smaller compared to total AOD. Therefore, requiring the standard deviation to be less than 0.01 may not be appropriate when assessing the representativeness of climatologies for aerosols separated into different types. The 17-year global mean optical depths over land for non-spherical, non-absorbing, and absorbing aerosols are about 0.077, 0.097, and 0.10, respectively. Given this, we applied AOD uncertainty criteria of 0.004, 0.005, and 0.005 for computing the minimum record lengths displayed in Figure 3b–d. The regional characteristics of minimum record lengths for speciated AOD (Figure 3b–d) tend to highlight the known climatological characteristics of these aerosol types. For example, persistent but highly variable dust plumes transported off western Africa and off the Arabian Peninsula lead to longer minimum record lengths for these regions. The Middle Eastern region affected by variable Shamal winds [37] also requires longer minimum record lengths. Interestingly, locations known primarily for biomass burning, including the equatorial region in Africa and equatorial South America, also appear to require longer minimum record lengths, though this might be due to the lack of the appropriate mixtures of dust and smoke in the MISR aerosol climatological lookup table [38]. The significantly longer minimum record length at high latitudes, most apparent in Figure 3b,d, is most likely related to the low quality of retrieved AOD over the regions due to cloud contamination [39].

Taken together, the non-absorbing and absorbing AOD maps shown in Figure 3c–d reflect the variability of biomass burning and anthropogenic industrial aerosols, because the retrievals of these components are complementary to one another. Besides the locations mentioned with respect to the total AOD in Figure 3a, the Atlantic Coast of the United States, and the Pacific downwind from the Hawaiian Islands stand out as requiring locally longer minimum record lengths. Figures A4–A7 in the Appendix show the same spatial patterns of the minimum record lengths as those in Figure 3, but for the four seasons. Not surprisingly, each seasonal mean AOD requires a longer sampling period to obtain a stable climatology compared to the annual mean AOD.

Figure 4 compares the minimum record lengths for total AOD derived from the MODIS retrievals for the high ($1° \times 1°$) and low ($5° \times 5°$) resolution datasets. When the MODIS AODs at $1°$ resolution are aggregated to $5°$ resolution, substantial information on spatial patterns in the original dataset is lost. Please note that the minimum record length required to achieve stability in the total MODIS AOD climatology at the higher resolution even exceeds 16 years in many parts of the world. This implies that even the full Terra data record of total AOD from MISR or MODIS may not be long enough to define a stable aerosol climatology at this resolution. This result is due to the larger variability of AOD at higher spatial resolution, which is not completely compensated by the more frequent sampling of MODIS than MISR.

The similarity between Figures 3a and 4b shows that the climatology from MODIS AOD remapped on MISR's grids is as stable as MISR AOD climatology despite differences in the retrieval algorithms and the sampling. To explore this further, Figure 4c shows the difference in the minimum record lengths between MISR and MODIS. Much of the map is red, indicating a longer required record length from MODIS than MISR, with the exception of the Amazon and the Congo, which experience significant biomass burning as well as frequent cloud cover. The fact that the record length is typically longer for MODIS than MISR is due to the aggregation of the higher resolution MODIS AOD retrievals to a coarser spatial resolution, which preserves some of the higher spatial variability. This is particularly apparent when considering the plume of aerosols downwind from the Hawaiian Islands that locally shows up as a larger enhancement in the minimum record length in the MODIS data (Figure 4b) than in the MISR data (Figure 3a). The Discussion section contains a more in-depth comparison of AOD time series between MISR and MODIS over the three green boxes in Figure 4c.
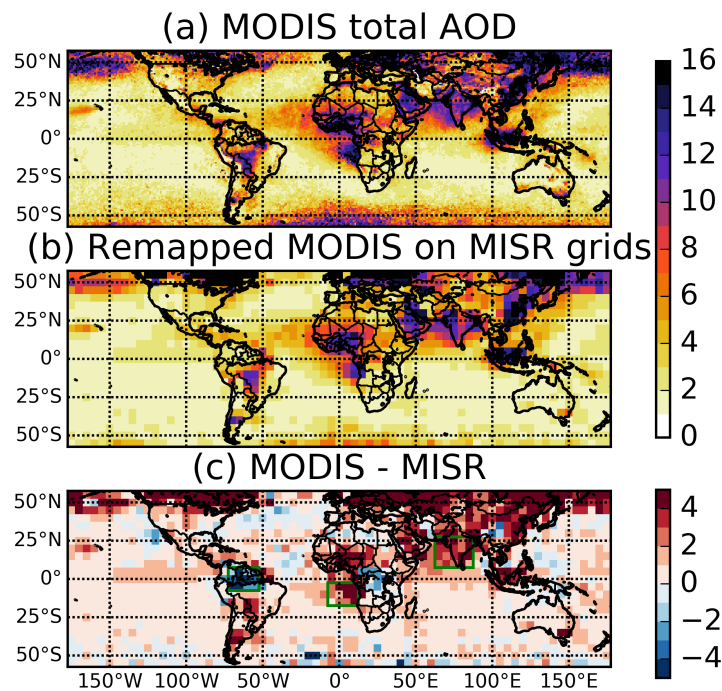
Figure 4. (**a**) The minimum record lengths required to obtain stable annual mean climatology of total AOD from MODIS within the accuracy level of ±0.01 AOD. (**b**) Same as (**a**) but the MODIS AOD dataset was remapped on MISR JOINT_AS' grid points. (**c**) The difference of the minimum record lengths in (**b**) with those from MISR in Figure 3).

Figure 5 summarizes the stability of MISR's speciated AOD climatologies for each season. The red lines in Figure 5 show the global median of the minimum record lengths required to obtain a sample standard deviation less than the predefined threshold (0.01 for total AOD, 0.004 for non-spherical AOD, and 0.005 for non-absorbing and absorbing AODs). Please note that each distribution represents the minimum record lengths quasi-globally (57.5° S–57.5° N) only over land to exclude the noisy signals over ocean at high latitudes. The blue boxes represent lower and upper quartiles of the minimum record lengths, so 75% of the data fall within these ranges. For the annual mean AOD, the global median value is about three years for the total MISR AOD and up to about seven years for the MISR absorbing AOD. These results provide confidence in the multi-year global mean AODs that have been used as proxies for the "climatological" AOD in previous studies using satellite data. Moreover, the results suggest that the MISR AOD observations over 17 years and its temporal subsets may provide enough information to examine global mean speciated AODs and, possibly, their radiative forcing with quantitative uncertainties (e.g., Xu et al. [40]).
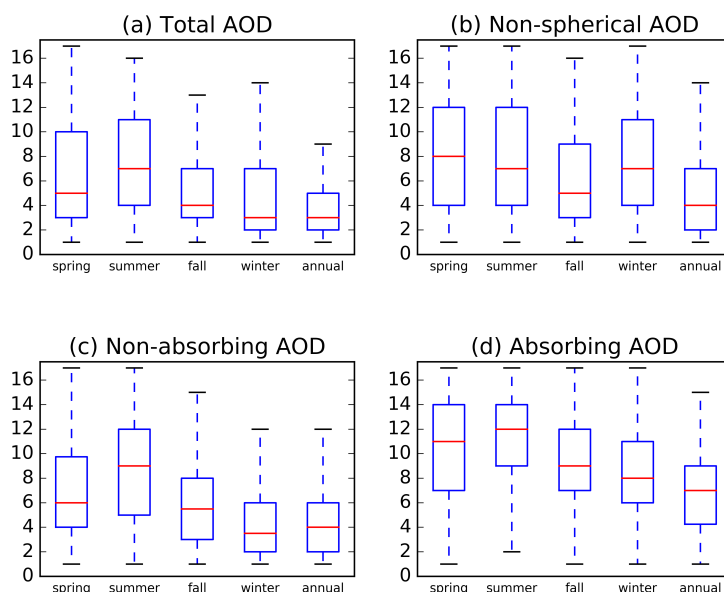
Figure 5. Spatial distributions of the minimum record lengths required to obtain stable climatology of (**a**) total, (**b**) non-spherical, (**c**) non-absorbing, and (**d**) absorbing aerosol optical depths for the four seasons and annual mean within the predefined accuracy levels (± 0.01 optical depth for total aerosols, ± 0.004 for nonspherical aerosols, and ± 0.005 for nonabsorbing and absorbing aerosols). Only the data over land were used.

To demonstrate the utility of considering aerosol climatologies with regard to their temporal subsampling, we evaluated three AEROCOM hindcast simulations focusing on the seasonal cycle of simulated AOD near two major sources of aerosol emissions: East China (22.5–42.5° N, 102.5–122.5° E) and the western coast of Africa to the west of the Sahara Desert (7.5–27.5° N, 42.5–22.5° W). The green boxes in Figure 6a display the two regions. The temporal overlap between the simulations and the MISR AOD retrievals is the five years from March 2000 through February 2005. The black bars in Figure 6b,c are area-mean total AOD from MISR for the two regions. The orange bars in Figure 6b represent non-absorbing AOD and in Figure 6c they represent non-spherical AOD. In East China, the uncertainty in 5-year mean non-absorbing AOD is less than 5% of the 17-year mean non-absorbing AOD in all four seasons. This also holds true for the uncertainty in non-spherical AOD west of the Sahara. The smaller orange error bars than black error bars indicate that even the 5-year mean AODs for non-absorbing and non-spherical aerosols for the two regions are as stable as their total AOD counterparts. In East China, the observed total AOD peaks in spring, whereas the non-absorbing AOD is highest in summer (Figure 6b). For this region, only the GOCART model accurately reproduces the observed seasonal cycles in the total and non-absorbing AOD fields, although GOCART and the other models all typically exhibit positive AOD biases relative to MISR in East China. To the west of the Sahara Desert, both total and non-spherical AODs peak in summer. In this case, the seasonal cycle is well represented in all three models. However, the total and non-spherical AODs from the models do not show very good quantitative agreement with the MISR observations. Although the three simulations were driven with the same dust emissions, the biases in the total and non-spherical AODs in HadGEM2 and SPRINTARS are negative for all four seasons and the annual mean, whereas those in GOCART are all positive. The quantitative uncertainties derived using our approach for the MISR-observed seasonal cycles of total and speciated AODs are smaller than the models' biases in both regions, thus ensuring a meaningful model evaluation.
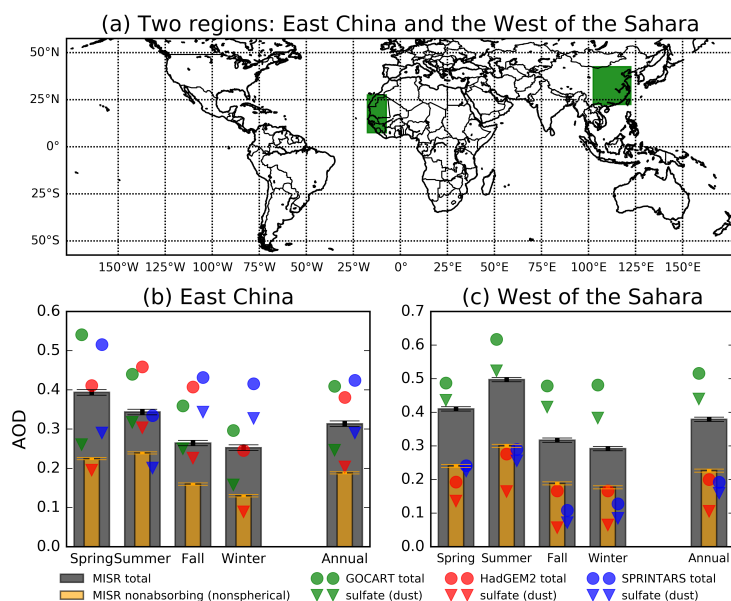
Figure 6. (**a**) Maps of the two regions, East China and west of the Sahara Desert. (**b**) Seasonal cycles and averages of total AOD (black bars) and non-absorbing AOD (orange bars) from MISR over East China. The error bars represent uncertainties due to the 5-year subsampling. The dots and triangles represent the corresponding total and nonabsorbing AOD from the three AEROCOM models. (**c**) Same as (**b**) but for total and non-spherical AOD in west of the Sahara Desert.

4. Discussion

The found difference in the stability of AOD climatologies between MISR and MODIS over several regions raises the question: what determines the stability? To answer this question, we compared the time series of annual mean AOD for the 17 years between MISR and MODIS over the three boxed regions in Figure 4c. Table 1 lists the mean and standard deviation of each time series in Figure 7 along with the minimum record length required to obtain a sample standard deviation less than 0.01. In Figure 7a, the time series represent AOD over land only in South America near the equator. On average, MODIS AOD (0.21) is slightly larger than MISR AOD (0.20) here, whereas standard deviation of MODIS AOD time series (i.e., the interannual variability) is lower than MISR. As a result, the climatology of MODIS AOD is more stable than MISR. In the other two regions, West Central Africa and India, both climatology and interannual variability in MODIS are higher than MISR. The larger MODIS AOD compared to MISR over India has been reported in many previous studies (e.g. Misra et al. [10], Ramachandran and Kedia [41], David et al. [42]). We show that AOD climatologies from MISR are also more stable than those from MODIS over these two regions. Figure 7 and Table 1 signify that the minimum record length represents interannual variability in AOD. It is interesting to note that AOD over ocean is greater than that over land in MODIS around India. In contrast, MISR's AOD is greater over land than ocean there. Understanding these differences in terms of their associated retrieval algorithms will require further work which is beyond the scope of this paper.
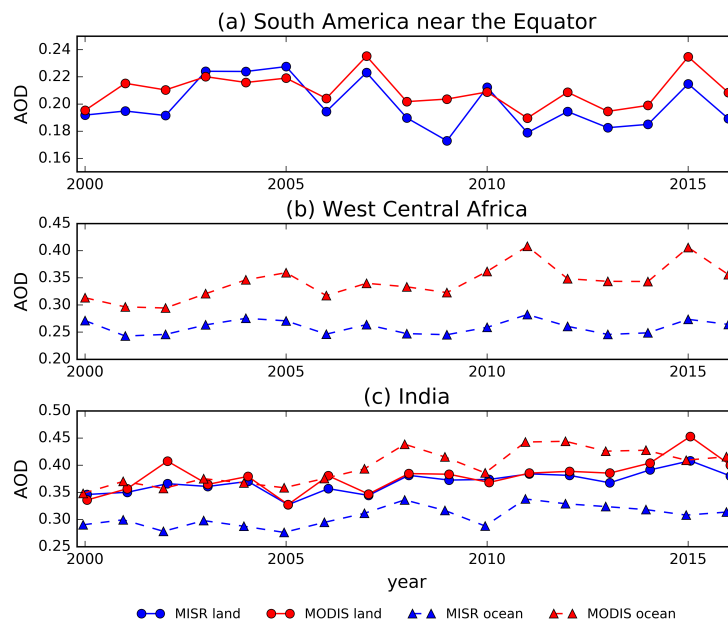
Figure 7. Time series of annual mean AODs from MISR (blue) and MODIS (red) between March 2000 and February 2017. The AODs on MISR JOINT_AS' grid points are spatially averaged over the three green boxes in Figure 4c. (**a**) South America near the Equator. (**b**) West Central Africa. (**c**) India. Solid and dotted lines represent AODs averaged over land and ocean respectively.

Table 1. The temporal mean and standard deviation (std.) of each time series in Figure 7, and the minimum record length (MRL) required to obtain a sample standard deviation less than 0.01.

Regions	MISR			MODIS		
	Mean	Std.	MRL	Mean	Std.	MRL
South America	0.2	0.017	3	0.21	0.012	2
West Central Africa	0.26	0.012	2	0.34	0.031	7
India (land)	0.37	0.019	4	0.38	0.029	6
India (ocean)	0.31	0.019	4	0.40	0.031	7

5. Conclusions

Satellite AOD retrievals are crucial for understanding aerosol distributions and their radiative effects on the Earth's climate system, and for validating these aspects in climate models. Prior to evaluating model simulated AODs against satellite observations, it is important to examine uncertainties in the multi-year mean AODs from satellite observations, which have been widely used for model evaluation.

We have shown that the length of satellite observation records affects the statistical stability of the climatological AOD, especially the AODs for different types of aerosols. Most importantly, our results show that the climatological AOD defined using a subset of MISR data for 17 years may be sufficiently stable on a global scale.

Our analysis demonstrates that continuing operations of MISR are essential to obtain more stable AOD climatologies by particle types. The aerosol type information from continuing MISR observations will further provide useful guidance to improve simulations of total aerosol loading and types in climate models. We stress that when evaluating AODs from models against satellite observations, it is important to check if the length of the observed AOD is longer than the minimum record length with a desired accuracy level.

Even so, there are regions, such as over the Sahara Desert (East China), where the climatological optical depth of dust (anthropogenic non-absorbing) aerosols is high, the uncertainties due to subsampling are small relative to the total AOD climatology. In addition, MISR's aerosol type information becomes relatively accurate and reliable in these regions where the total AOD typically exceeds 0.2 [25]. Although the difference between MISR and the AEROCOM models is larger than the uncertainty of multi-year mean AOD from MISR, one of the three models can reproduce the observed seasonal cycle of AOD in East China. In the west of the Sahara Desert, the three models have seasonal cycles similar to those in MISR.

Our methodology for estimating the minimum record length can be easily extended to other geophysical variables in the climate system. The minimum record length will be an especially useful quantity for researchers intending to use short-record satellite data for the purpose of model evaluation.

Author Contributions: Conceptualization, M.J.G., O.V.K. and H.L.; Methodology, H.L. and M.J.G.; Software, H.L.; Validation, M.J.G.; Formal Analysis, H.L.; Original Draft Preparation, H.L.; Review & Editing, M.J.G., O.V.K., Y.Y. and P.B.G.; Visualization, H.L.

Conflicts of Interest: The authors declare no conflict of interest.

Abbreviations

The following abbreviations are used in this manuscript:

MISR	Multi-angle Imaging SpectroRadiometer
AOD	Aerosol Optical Depth
WMO	World Meteorological Organization
EOS	Earth Observing System
AEROCOM	Aerosol Comparisons between Observations and Models
CMIP	Coupled Model Intercomparison Project
AerChemMIP	Aerosols and Chemistry Model Intercomparison Project
AERONET	Aerosol Robotic Network
Obs4MIPs	Observations for Model Intercomparions
JOINT_AS	Joint Aerosol Product
MODIS	Moderate resolution Imaging Spectroradiometer

Appendix A

The twelve maps in Figure A1 show the number of AOD retrievals used to estimate monthly mean AOD in JOINT_AS product in each month. Figures A2 and A3 display the confidence levels for AOD's linear trends and autocorrelation respectively. Figures A4–A7 show spatial patterns of the minimum years same as those in Figure 3, but for the four seasons.
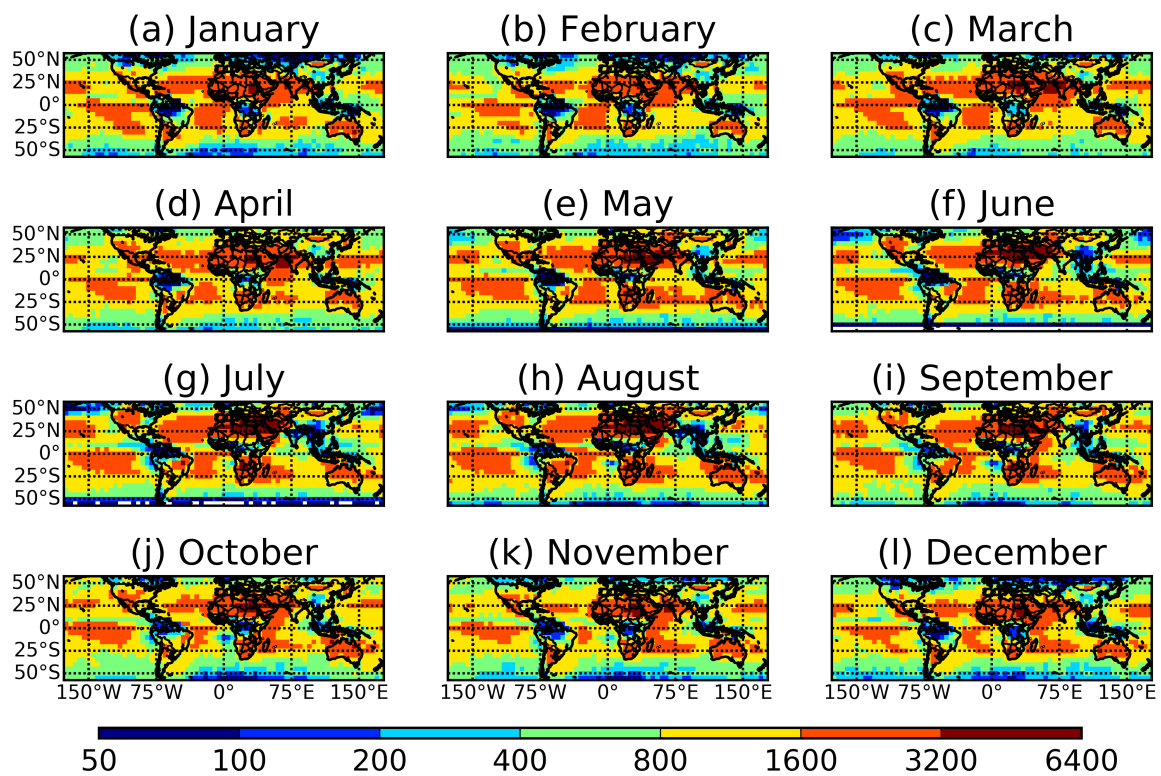
Figure A1. The number of AOD retrievals used to estimate monthly mean AOD in JOINT_AS product in each month. The values are averaged for the 17 years between March 2000 and February 2017.
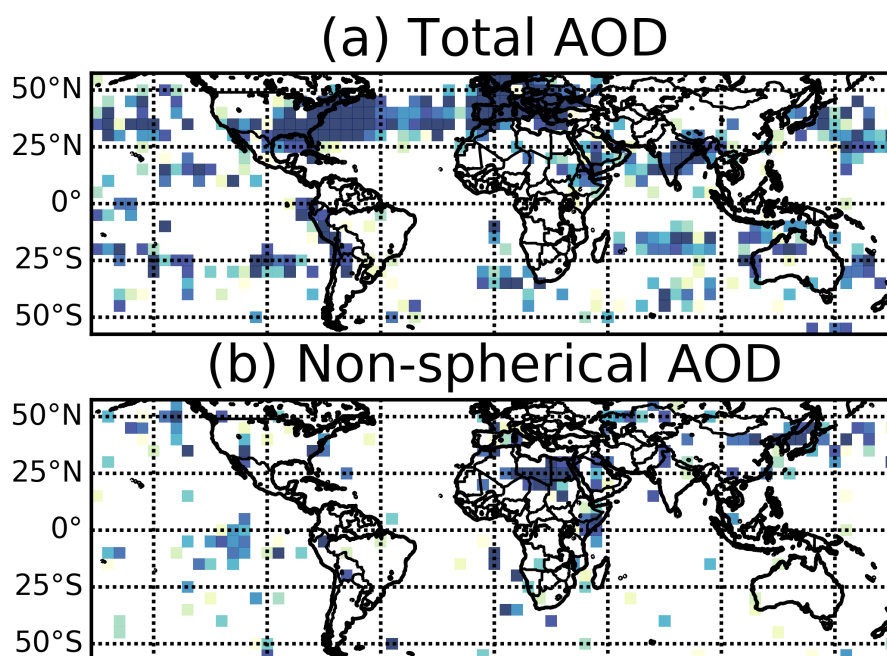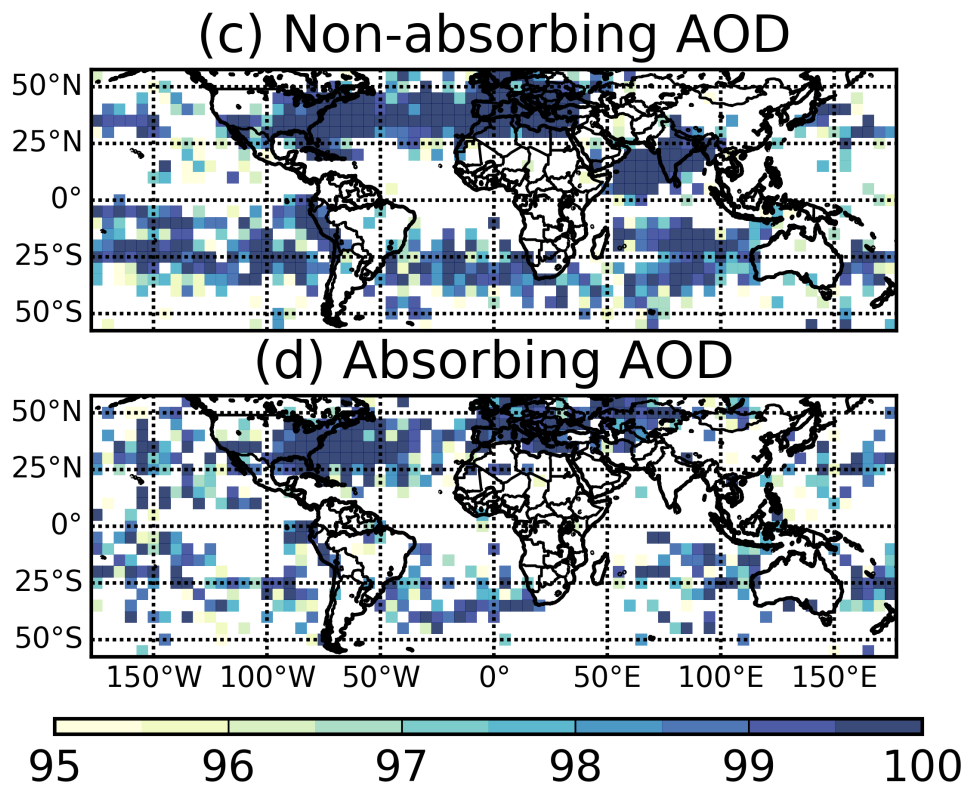

Figure A2. *Cont.*

Figure A2. Confidence levels (1- *p* value) in % for the slope of the least square lines fitting the time series of annual mean (**a**) total, (**b**) nonspherical, (**c**) nonabsorbing, and (**d**) absorbing aerosol optical depths during the 17 years between March 2000 and February 2017.
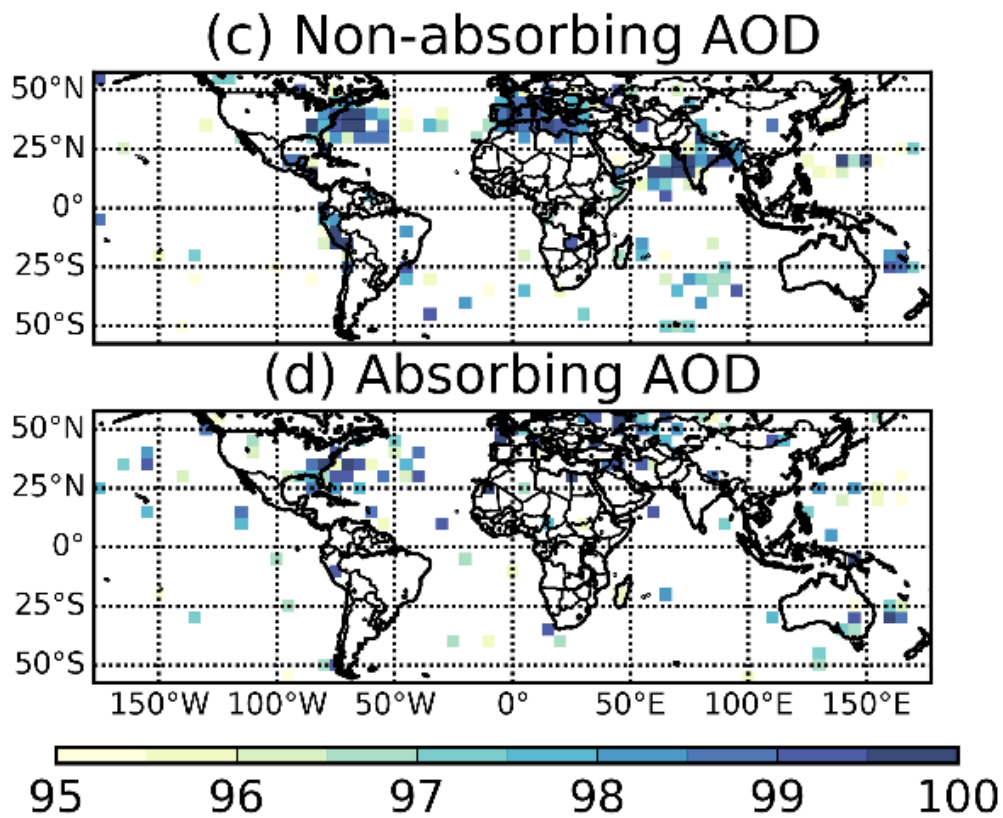

Figure A3. *Cont.*

(c) Non-absorbing AOD
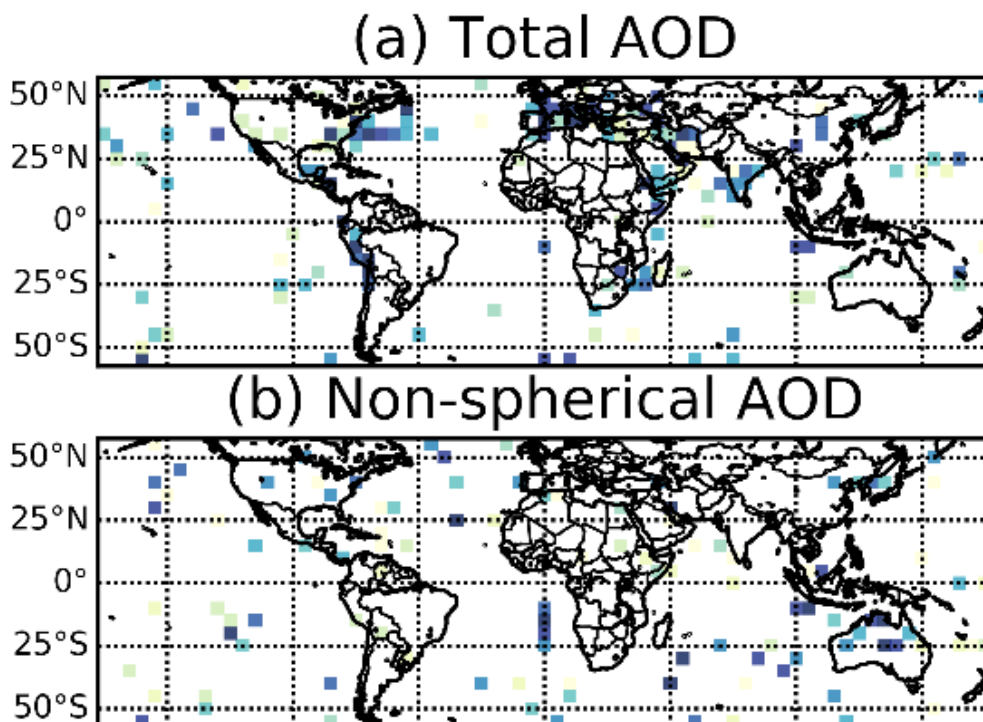
(d) Absorbing AOD

Figure A3. Confidence levels (1- *p* value) in % for lag 1-year autocorrelation in the time series of annual mean (**a**) total, (**b**) nonspherical, (**c**) nonabsorbing, and (**d**) absorbing aerosol optical depths during the 17 years between March 2000 and February 2017.
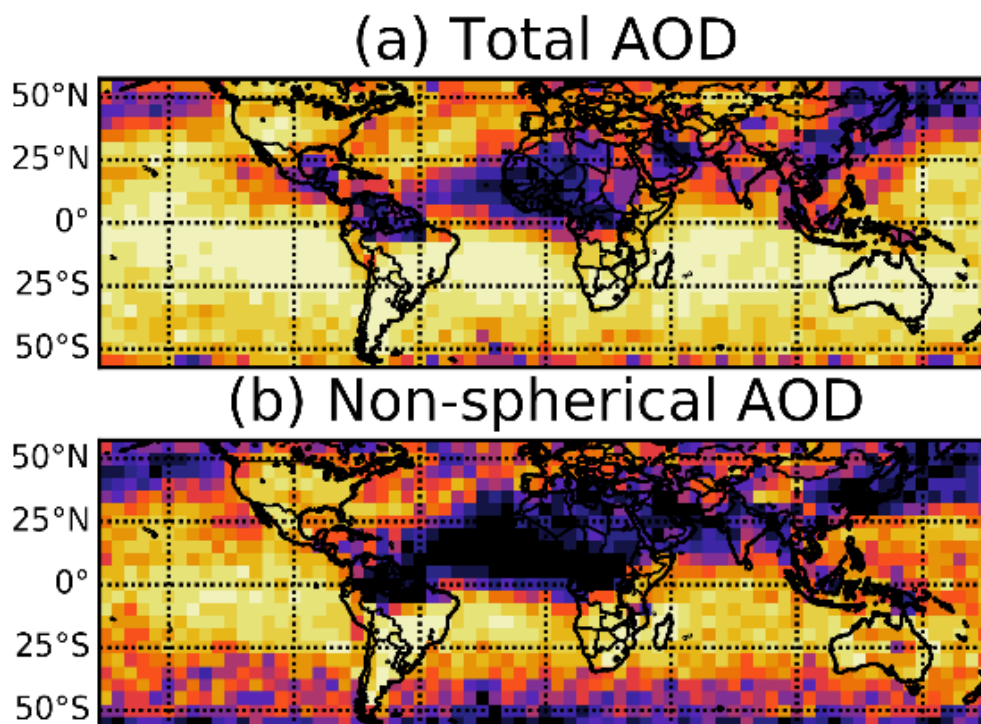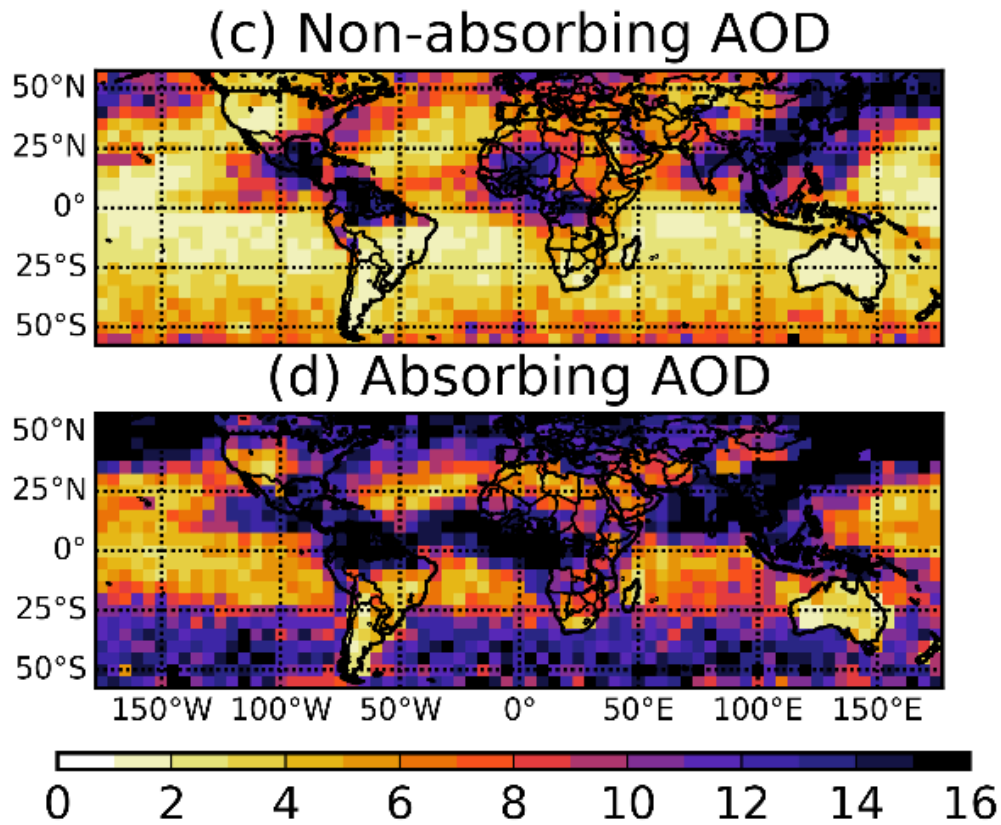
(a) Total AOD

(b) Non-spherical AOD

Figure A4. *Cont.*

Figure A4. The minimum record lengths required to obtain stable seasonal climatology of (**a**) total, (**b**) nonspherical, (**c**) nonabsorbing, and (**d**) absorbing aerosol optical depths in Spring (March-April-May) within the predefined accuracy levels (±0.01 AOD for (**a**), ±0.004 for (**b**), and ±0.005 for (**c**) and (**d**)).
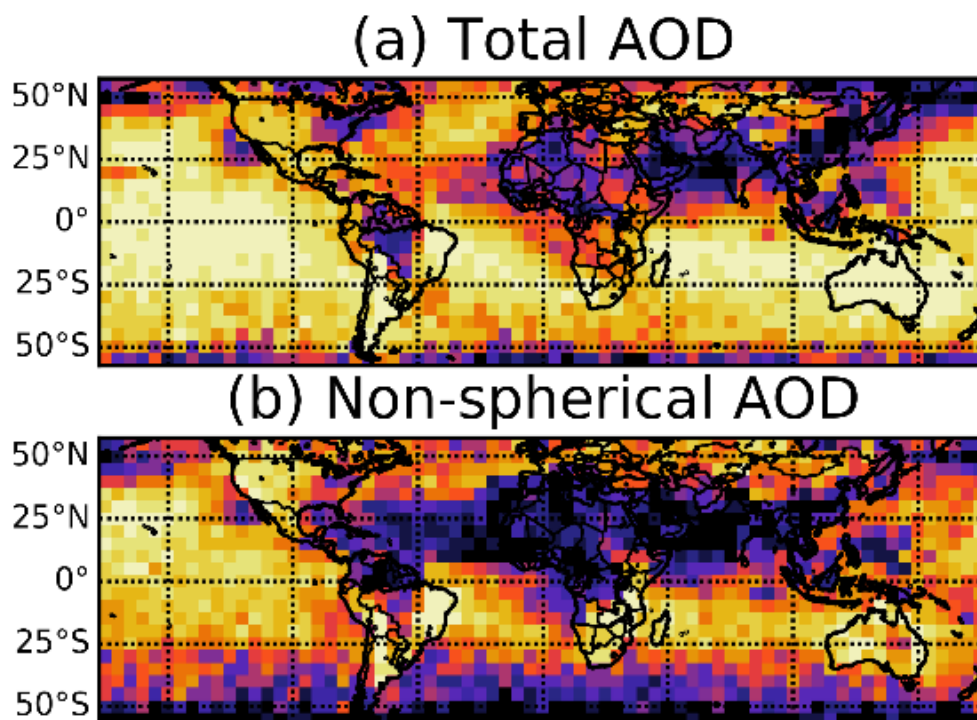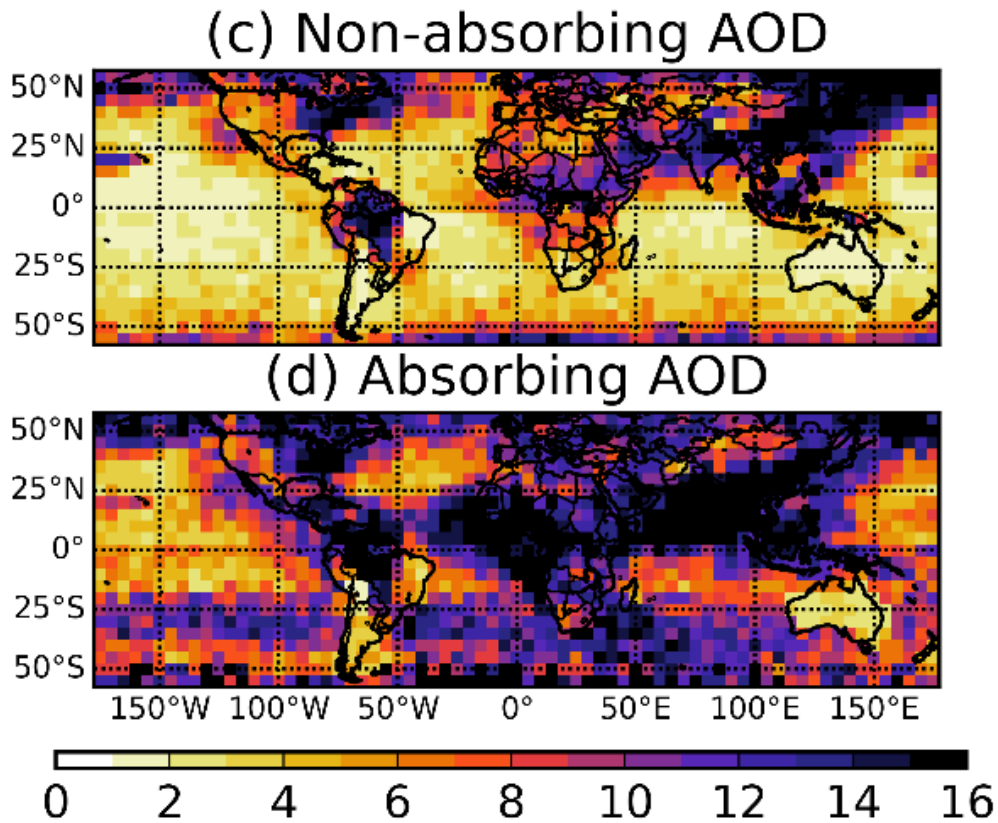

Figure A5. *Cont.*

Figure A5. The minimum record lengths required to obtain stable seasonal climatology of (**a**) total, (**b**) nonspherical, (**c**) nonabsorbing, and (**d**) absorbing aerosol optical depths in Summer (June-July-August) within the predefined accuracy levels ($\pm$0.01 AOD for (**a**), $\pm$0.004 for (**b**), and $\pm$0.005 for (**c**) and (**d**)).
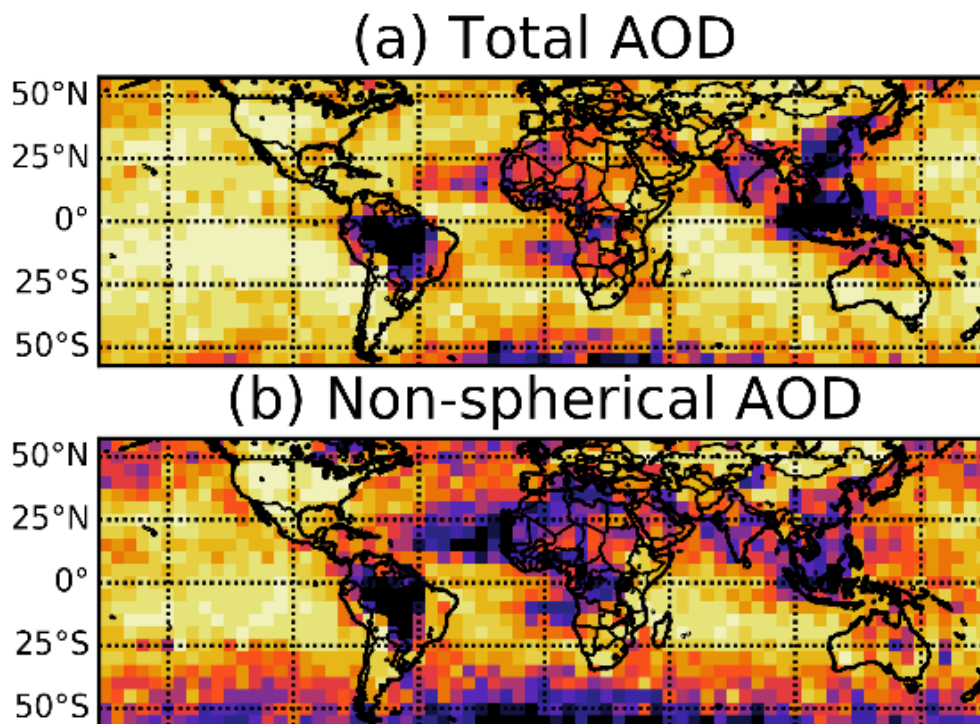

Figure A6. *Cont.*

Figure A6. The minimum record lengths required to obtain stable seasonal climatology of (**a**) total, (**b**) nonspherical, (**c**) nonabsorbing, and (**d**) absorbing aerosol optical depths in Fall (September-October-November) within the predefined accuracy levels (±0.01 AOD for (**a**), ±0.004 for (**b**), and ±0.005 for (**c**) and (**d**)).
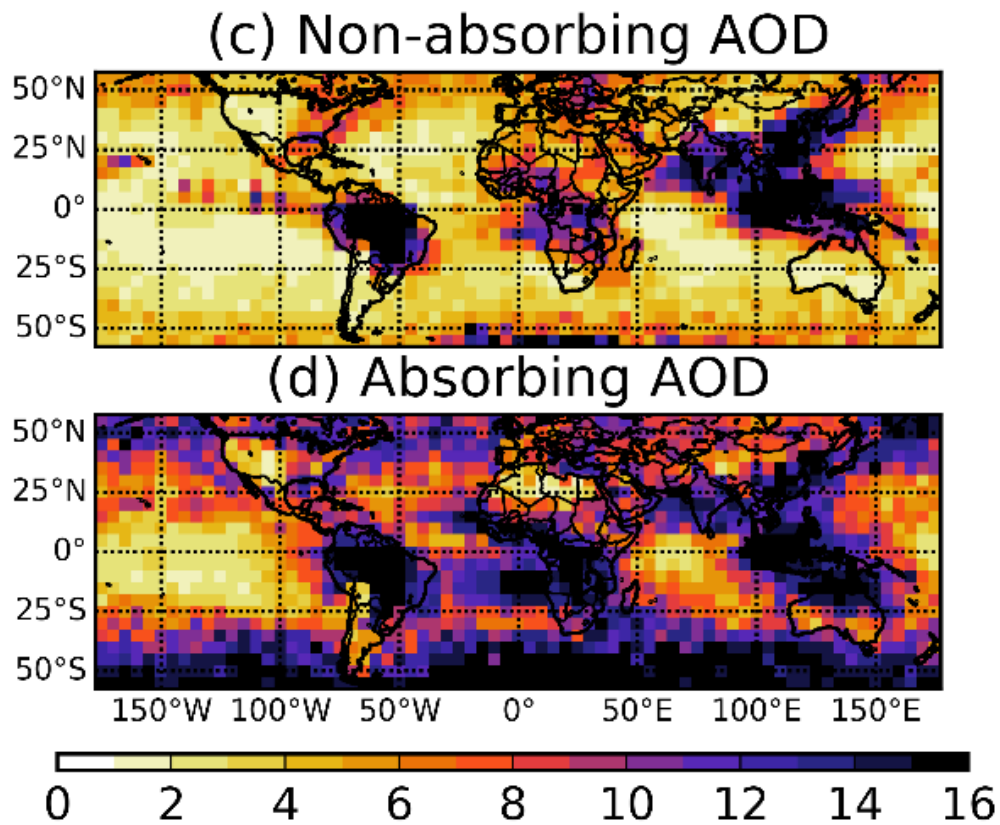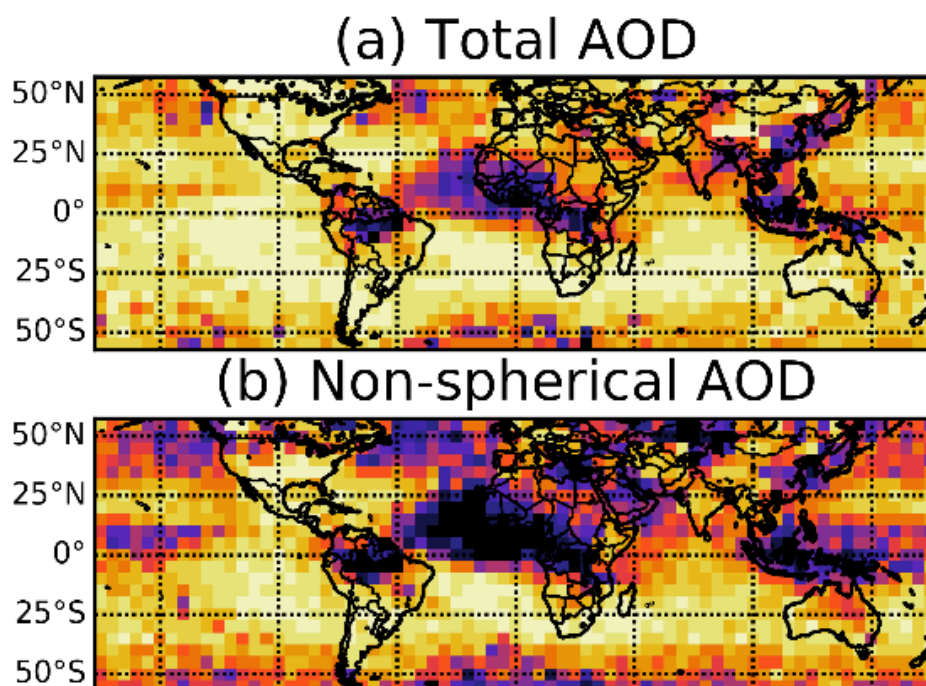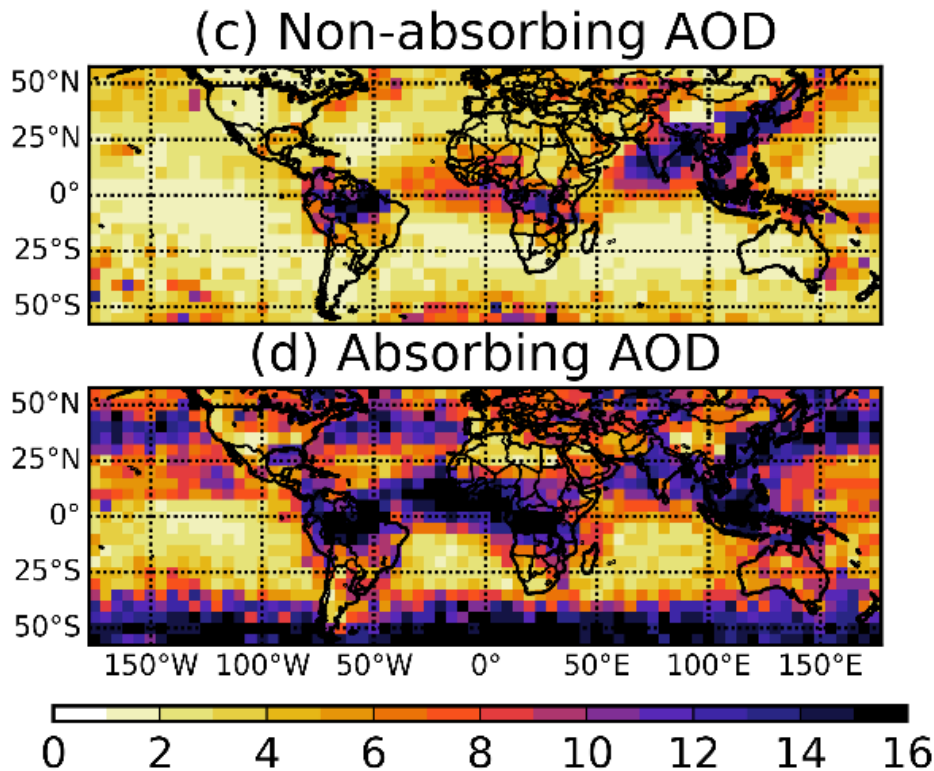

Figure A7. *Cont.*

Figure A7. The minimum record lengths required to obtain stable seasonal climatology of (**a**) total, (**b**) nonspherical, (**c**) nonabsorbing, and (**d**) absorbing aerosol optical depths in Winter (December-January-February) within the predefined accuracy levels (±0.01 AOD for (**a**), ±0.004 for (**b**), and ±0.005 for (**c**) and (**d**)).

References

1. IPCC (Intergovernmental Panel on Climate Change). *Climate Change 2013: The Physical Science Basis. Contribution of Working Group I to the Fifth Assessment Report of the Intergovernmental Panel on Climate Change*; Cambridge University Press: Cambridge, UK; New York, NY, USA, 2013; p. 1535, doi:10.1017/CBO9781107415324. [CrossRef]

2. Shindell, D.T.; Lamarque, J.F.; Schulz, M.; Flanner, M.; Jiao, C.; Chin, M.; Young, P.J.; Lee, Y.H.; Rotstayn, L.; Mahowald, N.; et al. Radiative forcing in the ACCMIP historical and future climate simulations. *Atmos. Chem. Phys.* **2013**, *13*, 2939–2974, doi:10.5194/acp-13-2939-2013. [CrossRef]

3. Park, H.; Chung, C.E.; Ekman, A.M.L.; Choi, J.O. Evaluation of ACCMIP simulated fine-mode AOD and its implication for aerosol direct forcing. *Asia Pac. J. Atmos. Sci.* **2014**, *50*, 377–390, doi:10.1007/s13143-014-0025-6. [CrossRef]

4. Pan, X.; Chin, M.; Gautam, R.; Bian, H.; Kim, D.; Colarco, P.R.; Diehl, T.L.; Takemura, T.; Pozzoli, L.; Tsigaridis, K.; et al. A multi-model evaluation of aerosols over South Asia: Common problems and possible causes. *Atmos. Chem. Phys.* **2015**, *15*, 5903–5928, doi:10.5194/acp-15-5903-2015. [CrossRef]

5. Zhu, J.; Xia, X.G.; Wang, J.; Che, H.Z.; Chen, H.B.; Zhang, J.Q.; Xu, X.G.; Levy, R.C.; Oo, M.; Holz, R.; et al. Evaluation of Aerosol Optical Depth and Aerosol Models from VIIRS Retrieval Algorithms over North China Plain. *Remote Sens.* **2017**, *9*, 432. doi:10.3390/rs9050432. [CrossRef] [PubMed]

6. Loew, A. Terrestrial satellite records for climate studies: How long is long enough? A test case for the Sahel. *Theor. Appl. Clim.* **2013**, *115*, 427–440, doi:10.1007/s00704-013-0880-6. [CrossRef]

7. Newman, M.; Alexander, M.A.; Ault, T.R.; Cobb, K.M.; Deser, C.; Di Lorenzo, E.; Mantua, N.J.; Miller, A.J.; Minobe, S.; Nakamura, H.; et al. The Pacific Decadal Oscillation, Revisited. *J. Clim.* **2016**, *29*, 4399–4427, doi:10.1175/Jcli-D-15-0508.1. [CrossRef]

8. Remer, L.A.; Kleidman, R.G.; Levy, R.C.; Kaufman, Y.J.; Tanre, D.; Mattoo, S.; Martins, J.V.; Ichoku, C.; Koren, I.; Yu, H.B.; et al. Global aerosol climatology from the MODIS satellite sensors. *J. Geophys. Res. Atmos.* **2008**, *113*, doi:10.1029/2007jd009661. [CrossRef]

9. Sreekanth, V. Satellite derived aerosol optical depth climatology over Bangalore, India. *Adv. Space Res.* **2013**, *51*, 2297–2308, doi:10.1016/j.asr.2013.01.022. [CrossRef]

10. Misra, A.; Kanawade, V.P.; Tripathi, S.N. Quantitative assessment of AOD from 17 CMIP5 models based on satellite-derived AOD over India. *Ann. Geophys.* **2016**, *34*, 657–671, doi:10.5194/angeo-34-657-2016. [CrossRef]

11. Aklesso, M.; Kumar, K.R.; Bu, L.B.; Boiyo, R. Analysis of spatial-temporal heterogeneity in remotely sensed aerosol properties observed during 2005–2015 over three countries along the Gulf of Guinea Coast in Southern West Africa. *Atmos. Environ.* **2018**, *182*, 313–324, [CrossRef]

12. Kumar, K.R.; Boiyo, R.; Madina, A.; Kang, N. A 13-year climatological study on the variations of aerosol and cloud properties over Kazakhstan from remotely sensed satellite observations. *J. Atmos. Solar Terr. Phys.* **2018**, *179*, 55–68, doi:10.1016/j.jastp.2018.06.014. [CrossRef]

13. Boiyo, R.; Kumar, K.R.; Zhao, T.L. Spatial variations and trends in AOD climatology over East Africa during 2002–2016: A comparative study using three satellite data sets. *Int. J. Clim.* **2018**, *38*, E1221–E1240. [CrossRef]

14. Hu, K.; Kumar, K.R.; Kang, N.; Boiyo, R.; Wu, J.W. Spatiotemporal characteristics of aerosols and their trends over mainland China with the recent Collection 6 MODIS and OMI satellite datasets. *Environ. Sci. Pollut. Res.* **2018**, *25*, 6909–6927. [CrossRef] [PubMed]

15. Lee, H.; Kalashnikova, O.V.; Suzuki, K.; Braverman, A.; Garay, M.J.; Kahn, R.A. Climatology of the aerosol optical depth by components from the Multi-angle Imaging SpectroRadiometer (MISR) and chemistry transport models. *Atmos. Chem. Phys.* **2016**, *16*, 6627–6640, doi:10.5194/acp-16-6627-2016. [CrossRef]

16. Tsigaridis, K.; Daskalakis, N.; Kanakidou, M.; Adams, P.J.; Artaxo, P.; Bahadur, R.; Balkanski, Y.; Bauer, S.E.; Bellouin, N.; Benedetti, A.; et al. The AeroCom evaluation and intercomparison of organic aerosol in global models. *Atmos. Chem. Phys.* **2014**, *14*, 10845–10895, doi:10.5194/acp-14-10845-2014. [CrossRef]

17. Myhre, G.; Samset, B.H.; Schulz, M.; Balkanski, Y.; Bauer, S.; Berntsen, T.K.; Bian, H.; Bellouin, N.; Chin, M.; Diehl, T.; et al. Radiative forcing of the direct aerosol effect from AeroCom Phase II simulations. *Atmos. Chem. Phys.* **2013**, *13*, 1853–1877, doi:10.5194/acp-13-1853-2013. [CrossRef]

18. Eyring, V.; Bony, S.; Meehl, G.A.; Senior, C.A.; Stevens, B.; Stouffer, R.J.; Taylor, K.E. Overview of the Coupled Model Intercomparison Project Phase 6 (CMIP6) experimental design and organization. *Geosci. Model Dev.* **2016**, *9*, 1937–1958, doi:10.5194/gmd-9-1937-2016. [CrossRef]

19. Diner, D.J.; Beckert, J.C.; Reilly, T.H.; Bruegge, C.J.; Conel, J.E.; Kahn, R.A.; Martonchik, J.V.; Ackerman, T.P.; Davies, R.; Gerstl, S.A.W.; et al. Multi-angle Imaging SpectroRadiometer (MISR) - Instrument description and experiment overview. *IEEE Trans. Geosci. Remote Sens.* **1998**, *36*, 1072–1087, doi:10.1109/36.700992. [CrossRef]

20. Diner, D.J.; Martonchik, J.V.; Kahn, R.A.; Pinty, B.; Gobron, N.; Nelson, D.L.; Holben, B.N. Using angular and spectral shape similarity constraints to improve MISR aerosol and surface retrievals over land. *Remote Sens. Environ.* **2005**, *94*, 155–171, doi:10.1016/j.rse.2004.09.009. [CrossRef]

21. Chin, M.; Diehl, T.; Tan, Q.; Prospero, J.M.; Kahn, R.A.; Remer, L.A.; Yu, H.; Sayer, A.M.; Bian, H.; Geogdzhayev, I.V.; et al. Multi-decadal aerosol variations from 1980 to 2009: A perspective from observations and a global model. *Atmos. Chem. Phys.* **2014**, *14*, 3657–3690, doi:10.5194/acp-14-3657-2014. [CrossRef]

22. Collins, W.J.; Bellouin, N.; Doutriaux-Boucher, M.; Gedney, N.; Hinton, T.; Jones, C.D.; Liddicoat, S.; Martin, G.; O'Connor, F.; Rae, J.; et al. *Evaluation of the HadGEM2 Model*; Met Office Hadley Centre Technical Note No. HCTN 74; Met Office: Exeter, UK, 2008.

23. Takemura, T.; Nozawa, T.; Emori, S.; Nakajima, T.Y.; Nakajima, T. Simulation of climate response to aerosol direct and indirect effects with aerosol transport-radiation model. *J. Geophys. Res. Atmos.* **2005**, *110*, doi:10.1029/2004jd005029. [CrossRef]

24. Kahn, R.A.; Gaitley, B.J.; Garay, M.J.; Diner, D.J.; Eck, T.F.; Smirnov, A.; Holben, B.N. Multiangle Imaging SpectroRadiometer global aerosol product assessment by comparison with the Aerosol Robotic Network. *J. Geophys. Res. Atmos.* **2010**, *115*, doi:10.1029/2010jd014601. [CrossRef]

25. Kahn, R.A.; Gaitley, B.J. An analysis of global aerosol type as retrieved by MISR. *J. Geophys. Res. Atmos.* **2015**, *120*, 4248–4281, doi:10.1002/2015jd023322. [CrossRef]

26. Garay, M.J.; Kalashnikova, O.V.; Bull, M.A. Development and assessment of a higher-spatial-resolution (4.4 km) MISR aerosol optical depth product using AERONET-DRAGON data. *Atmos. Chem. Phys.* **2017**, *17*, 5095–5106, doi:10.5194/acp-17-5095-2017. [CrossRef]

27. Holben, B.N.; Eck, T.F.; Slutsker, I.; Tanre, D.; Buis, J.P.; Setzer, A.; Vermote, E.; Reagan, J.A.; Kaufman, Y.J.; Nakajima, T.; et al. AERONET—A federated instrument network and data archive for aerosol characterization. *Remote Sens. Environ.* **1998**, *66*, 1–16, doi:10.1016/S0034-4257(98)00031-5. [CrossRef]

28. Kin, S.; O'Donnel, D.; Stier, P.; Kloster, S.; Zhang, K.; Schmidt, H.; Rast, S.; Giorgetta, M.; Eck, T.F.; Stevens, B. MAC-v1: A new global aerosol climatology for climate studies. *J. Adv. Model. Earth Syst.* **2013**, *5*, 704–740, doi:10.1002/jame.20035. [CrossRef]

29. Teixeira, J.; Waliser, D.; Ferraro, R.; Gleckler, P.; Lee, T.; Potter, G. Satellite Observations for CMIP5 The Genesis of Obs4MIPs. *Bull. Am. Meteorol. Soc.* **2014**, *95*, 1329–1334, doi:10.1175/Bams-D-12-00204.1. [CrossRef]

30. Ferraro, R.; Waliser, D.E.; Gleckler, P.; Taylor, K.E.; Eyring, V. Evolving Obs4MIPs to Support Phase 6 of the Coupled Model Intercomparison Project (CMIP6). *Bull. Am. Meteorol. Soc.* **2015**, *96*, Es131–Es133, doi:10.1175/Bams-D-14-00216.1. [CrossRef]

31. Lee, H.; Jeong, S.J.; Kalashnikova, O.; Tosca, M.; Kim, S.W.; Kug, J.S. Characterization of Wildfire-Induced Aerosol Emissions From the Maritime Continent Peatland and Central African Dry Savannah with MISR and CALIPSO Aerosol Products. *J. Geophys. Res. Atmos.* **2018**, *123*, 3116–3125, doi:10.1002/2017jd027415. [CrossRef]

32. Ichoku, C.; Ellison, L. Global top-down smoke-aerosol emissions estimation using satellite fire radiative power measurements. *Atmos. Chem. Phys.* **2014**, *14*, 6643–6667. [CrossRef]

33. Brockwell, J.P. *Introduction to Time Series and Forecasting*; Springer Science+Business Media: New York, NY, USA, 2016.

34. Lee, H.; Waliser, D.E.; Ferraro, R.and Iguchi, T.; Peters-Lidard, C.D.; Tian, B.; Loikith, P.C.; Wright, D.B. Evaluating hourly rainfall characteristics over the U.S. Great Plains in dynamically downscaled climate model simulations using NASA-Unified WRF. *J. Geophys. Res. Atmos.* **2017**, doi:10.1002/2017jd026564. [CrossRef]

35. Levy, R.C.; Mattoo, S.; Munchak, L.A.; Remer, L.A.; Sayer, A.M.; Patadia, F.; Hsu, N.C. The Collection 6 MODIS aerosol products over land and ocean. *Atmos. Meas. Tech.* **2013**, *6*, 2989–3034, doi:10.5194/amt-6-2989-2013. [CrossRef]

36. Hsu, N.C.; Tsay, S.C.; King, M.D.; Herman, J.R. Deep blue retrievals of Asian aerosol properties during ACE-Asia. *IEEE Trans. Geosci. emote Sens.* **2006**, *44*, 3180–3195, doi:10.1109/Tgrs.2006.879540. [CrossRef]

37. Yu, Y.; Notaro, M.; Kalashnikova, O.V.; Garay, M.J. Climatology of summer Shamal wind in the Middle East. *J. Geophys. Res. Atmos.* **2016**, *121*, 289–305, doi:10.1002/2015jd024063. [CrossRef]

38. Kahn, R.A.; Nelson, D.L.; Garay, M.J.; Levy, R.C.; Bull, M.A.; Diner, D.J.; Martonchik, J.V.; Paradise, S.R.; Hansen, E.G.; Remer, L.A. MISR Aerosol Product Attributes and Statistical Comparisons With MODIS. *IEEE Trans. Geosci. Remote Sens.* **2009**, *47*, 4095–4114, doi:10.1109/tgrs.2009.2023115. [CrossRef]

39. Shi, Y.; Zhang, J.; Reid, J.S.; Liu, B.; Hyer, E.J. Critical evaluation of cloud contamination in the MISR aerosol products using MODIS cloud mask products. *Atmos. Meas. Tech.* **2014**, *7*, 1791–1801, doi:10.5194/amt-7-1791-2014. [CrossRef]

40. Xu, H.; Ceamanos, X.; Roujean, J.L.; Carrer, D.; Xue, Y. Can satellite-derived aerosol optical depth quantify the surface aerosol radiative forcing? *Atmos. Res.* **2014**, *150*, 151–167, doi:10.1016/j.atmosres.2014.07.008. [CrossRef]

41. Ramachandran, S.; Kedia, S. Aerosol Optical Properties over South Asia from Ground-Based Observations and Remote Sensing: A Review. *Climate* **2013**, *1*, 84–119, doi:10.3390/cli1030084. [CrossRef]

42. David, L.M.; Ravishankara, A.R.; Kodros, J.K.; Venkataraman, C.; Sadavarte, P.; Pierce, J.R.; Chaliyakunnel, S.; Millet, D.B. Aerosol Optical Depth Over India. *J. Geophys. Res. Atmos.* **2018**, *123*, 3688–3703, doi:10.1002/2017jd027719. [CrossRef]